

Frequency-dependent cables and overhead lines for the calculation of short-circuit currents of HVDC converters

A. Wasserrab, G. Balzer

Abstract—In this paper the DC short-circuit current of HVDC converters under consideration of frequency-dependent overhead lines and cables is analyzed. At a DC short circuit the transient and steady-state short-circuit currents are determined by the characteristics of the AC and DC system. The different influence factors are shortly introduced here. In particular the overhead line or cable section between HVDC converter and fault location influences the peak short-circuit current and time to peak of the converter contribution. The total short-circuit current at the fault location is the superposition of the converter and the line discharge current. In addition to the converter short-circuit current the discharge current of the line is evaluated. In several HVDC system scenarios – with different DC line configurations – short-circuit currents based on frequency-dependent lines are compared to them of simplified line models convenient for short-circuit current calculation methods. The paper concludes with recommendations for the consideration of DC lines in short-circuit current calculation methods .

Keywords: cable, frequency-dependence, HVDC, overhead line, short circuit, short-circuit current.

I. INTRODUCTION

THE first HVDC system was put into operation 60 years ago. Since the beginning almost all systems – with a few exceptions – were realized as point-to-point connections. With the development of self-commutated converters so-called multi-terminal systems with a high number of converter terminals became feasible. It is expected that multi-terminal systems will be realized in the future for example offshore to connect several wind farms to the grid [1]. Such DC grids have to be dimensioned according to the maximum DC short-circuit currents. Calculation methods for DC short-circuit currents are therefore needed to be standardized similar to IEC 60909-0 for AC systems [2].

Voltage source converters (VSC) will be the technology of choice for prospective DC grids as mentioned above. The first self-commutated systems were based on two-level VSCs. A few years ago a new converter type called modular multi-level converter (MMC) emerged, which is very promising because

of a small footprint and low losses [3]. In general, it can be distinguished between MMC with half-bridge and full-bridge submodules. The analysis here focuses on MMCs with half-bridge submodules. Converters with full-bridge submodules are less relevant for short-circuit current calculation methods, because of the ability to reduce the fault current to zero by control action [4].

HVDC converter stations are connected either by cables or overhead lines. Their impedance depends naturally on the frequency because of the skin effect of the conductor and earth. In the steady state only the resistance of the respective line is effective. In case of a DC short circuit the transient behavior of the line has to be considered.

The simulation environment PSCAD[®] provides frequency-dependent line models as the *Phase* or *Mode Model*, which give the exact time response after a transient event [5]. From a short-circuit current calculation point of view such elaborate models are not convenient for the determination of characteristic short-circuit parameters as the peak short-circuit current, steady-state short-circuit current and time to peak. Therefore, in prospective short-circuit current calculation methods for HVDC grids it has to be specified how the frequency-dependent overhead line or cable has to be considered.

In section II the short-circuit current of an HVDC converter is analyzed. Additionally, the influence factors, which determine the converter short-circuit currents are discussed. Section III covers the short-circuit current of the line. Here the different frequency-dependent line models are introduced. In section IV the simulation model and results for different scenarios are presented.

II. CONVERTER SHORT-CIRCUIT CURRENT

At a short circuit in the DC system the IGBTs of MMC half-bridge submodules are blocked. In this case the short-circuit current – fed from the AC system – flows over the submodule diodes to the DC side. The equivalent circuit of a monopolar MMC in the short-circuit state is shown in Fig. 1.

The parameters R_{ac} and L_{ac} represent the inductance and resistance of the AC system. They are mainly determined by the strength of the AC infeed, characterized by the initial short-circuit current I_k of the grid, and the converter transformer. Typical short-circuit voltages of the transformer impedance are around 0.15 p.u. Two-level VSCs have additional converter reactances for control purposes.

Andreas Wasserrab and Gerd Balzer are with the Department of Electrical Power Systems, Technische Universität Darmstadt, Germany (e-mail: andreas.wasserrab@eev.tu-darmstadt.de and gerd.balzer@eev.tu-darmstadt.de).

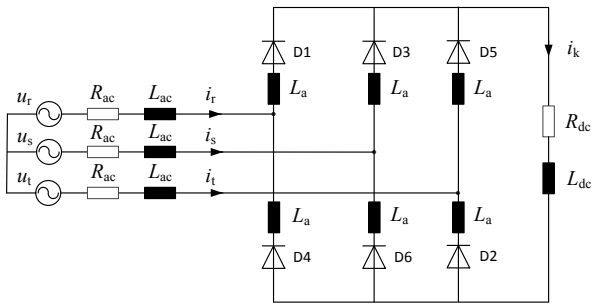


Fig. 1. Equivalent circuit of a modular multi-level converter in the short-circuit state (monopolar).

In case of an MMC arm inductances are applied instead, which decrease the resulting short-circuit current. The arm inductances are represented by the parameter L_a in the equivalent circuit. On the DC side the short-circuit current is influenced by the characteristics of the DC line. For the analysis of the converter short-circuit current the line is represented here by its lumped series parameters R_{dc} and L_{dc} . The capacitance of the line is neglected.

In the short-circuit state at least three diodes are conducting at the same time. Assuming a state with the conducting diodes D3, D4 and D5 the following differential equation can be derived, which is valid for the duration of that commutation state:

$$i_k R_k + \frac{di_k}{dt} L_k = -\hat{u} \sin(\omega t) \quad (1)$$

with

$$L_k = L_{ac} + L_a + \frac{2}{3} L_{dc} \quad (2)$$

$$R_k = R_{ac} + \frac{2}{3} R_{dc} \quad (3)$$

In case of other commutation states with three conducting diodes only the right side of (1) has to be adapted. The solution for i_k is (initial conditions are zero):

$$i_k = -\frac{\hat{u}}{R_k^2 + (\omega L_k)^2} \left[R_k \sin(\omega t) - \omega L_k \cos(\omega t) + \omega L_k e^{-\frac{R_k t}{L_k}} \right] \quad (4)$$

The short-circuit current consists of a steady-state component with fundamental frequency and a decaying DC component. The time-course for the whole short-circuit duration results from the superposition of the time-shifted partial currents according to (4) and the corresponding solutions for the different commutation states. If four or five diodes are conducting simultaneously the frequency-components are the same as in (4), but the solution for i_k is more elaborate, because of the voltage drop on L_a . In case of six conducting diodes i_k consists only of a decaying DC component.

A typical time-course of a converter short-circuit current is shown in Fig. 2. It is characterized here by the parameters peak short-circuit current i_p (maximum amplitude of the short-circuit current), steady-state short-circuit current I_k and time to peak t_p . These parameters are calculated based on the parameters depicted in Fig. 1. If the arm inductance is neglected the calculation method described in [6] can be applied.

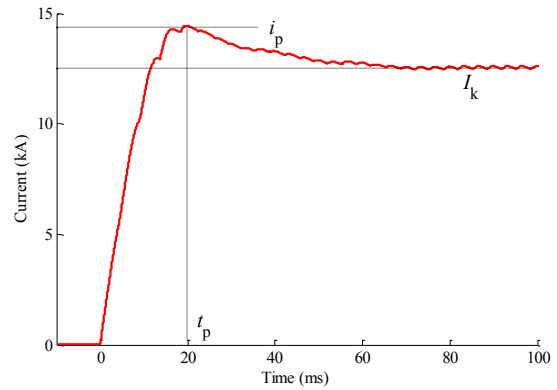


Fig. 2. Typical time-course of a converter short-circuit current.

An approach considering additionally L_a for the calculation of the characteristic short-circuit current parameters can be found in [7].

As the line parameters depend generally on the frequency, it has to be determined, which frequency has to be applied for the calculation of R_{dc} and L_{dc} .

III. LINE SHORT-CIRCUIT CURRENT

At a short circuit in an HVDC system the overhead line or cable influences the short-circuit current in two ways: Firstly, the line impedance between converter terminal and fault location effects directly the amplitude of the converter short-circuit current. Secondly, the line is discharged and contributes to the total short-circuit current in addition to the converter.

In subsection A the different distributed line models are presented, which are applied in PSCAD[®]. Subsection B describes the calculation of frequency-dependent line parameters and finally in subsection C the discharge current of frequency-dependent lines is analyzed.

A. Line Models

The simulation environment PSCAD[®] provides three different distributed line models. The *Bergeron Model* is based on distributed LC -parameters. The losses are considered as lumped elements at the middle and the ends of the line. For that model the line parameters are calculated for a single frequency. The *Frequency-Dependent (Mode or Phase) Model* instead represents the frequency behavior over a specified frequency range. All the parameters – R , L and C – are distributed along the line. The *Mode Model* applies a frequency-independent modal transformation matrix to decouple the original system into separate modes. The *Phase Model* considers additionally the frequency-dependence of internal transformation matrices, which is more accurate [5]. In the following simulations the *Phase Model* is applied.

B. Line Parameters

The electrical behavior of a line is described by its series impedance \underline{Z} and shunt admittance \underline{Y} per unit length. The calculation of both parameters is described in [8] for the overhead line and in [9] for the cable. The series impedance depends on the frequency, because of the skin effect in the conductor and earth.

Table I contains specifications of a 320 kV HVDC cable with XLPE insulation and a 500 kV HVDC overhead line, which are used as reference models for the analyses. The cable sheath is grounded at both ends.

The calculated resistance R' and inductance L' per unit length in dependence of the frequency for the overhead line and cable are shown in Fig. 3. and Fig 4. For both types monopolar (with earth return) and bipolar line configurations are considered. In case of the bipolar configuration it is assumed that the short-circuit current flows down one conductor and back on the other one, which corresponds to the metallic propagation mode.

TABLE I
HVDC CABLE AND OVERHEAD LINE SPECIFICATIONS

HVDC Cable (XLPE)	
Conductor	Cu, 2500 mm ² , $r_1 = 28$ mm
Inner insulation	$\epsilon_1 = 2.5$, $r_2 = 54$ mm
Sheath	Pb, $r_3 = 59$ mm
Outer insulation	$\epsilon_2 = 2.4$, $r_4 = 64$ mm
Cable depth	$h = 1.2$ m
Distance centre points (bipolar)	$d = 0.3$ m
HVDC Overhead Line	
Conductor	Al/St 2x 645/45, $\rho_c = 2.9 \cdot 10^{-8}$ Ω m
Conductor height	$h = 38$ m, $sag = 17.5$ m
Distance centre points (bipolar)	$d = 13.4$ m
Earth	$\rho_e = 100$ Ω m

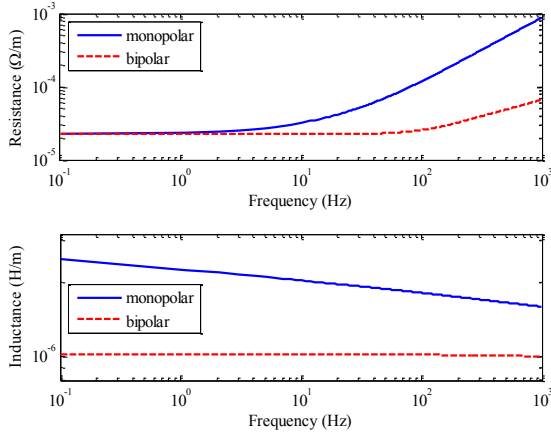


Fig. 3. Resistance and inductance per unit length of an overhead line.

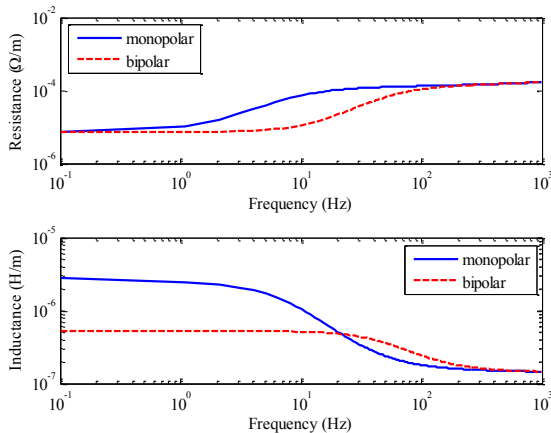


Fig. 4. Resistance and inductance per unit length of a cable.

As can be seen in Fig. 3 for the monopolar overhead line configuration the resistance increases and the inductance decreases with increasing frequency. The parameters of the bipolar configuration are almost constant over the whole frequency range. The reason is that the earth impedance – which depends highly on the frequency – has no effect on the resulting impedance in case of a bipolar configuration at a line-to-line short circuit. The parameters of the monopolar cable configuration show a similar tendency in dependence of the frequency as the parameters of the monopolar overhead line (see Fig. 4). The parameters of the bipolar configuration are also frequency-dependent in particular for frequencies above 10 Hz, because of the influence of the sheath.

Based on the parameters per unit length the surge impedance Z_w and propagation constant γ are determined:

$$Z_w = \sqrt{\frac{Z'}{Y'}} \quad (5)$$

$$\gamma = \sqrt{Z' \cdot Y'} = \alpha + j\beta \quad (6)$$

Where α is the damping constant and β the phase constant of the line. The propagation of traveling waves along the line is described by those parameters.

The calculation of converter short-circuit currents according to [6], [7] requires lumped elements as depicted in Fig. 1 to determine characteristic short-circuit current parameters. For a single frequency the equivalent parameters of a distributed line are calculated as follows:

$$\underline{Z} = \underline{Z}_w \sinh(\underline{\gamma}l) = R + j\omega L \quad (7)$$

$$\underline{Y} = \frac{1}{\underline{Z}_w} \tanh(\underline{\gamma}l) = G + j\omega C \quad (8)$$

Where \underline{Z} is the series impedance and \underline{Y} the shunt admittance of a π -equivalent circuit. For short lines the shunt admittance can be omitted at a short circuit. In section IV the differences between a simplified approach with lumped elements according to (7) and a detailed frequency-dependent model as described in subsection A are evaluated.

C. Discharge Current

At a short circuit in an HVDC system lines are discharged. The amount of energy stored in the line depends on the line capacitance C and the instantaneous DC voltage U_{dc} :

$$W = \frac{1}{2} C \cdot U_{dc}^2 \quad (9)$$

The initial amplitude of the discharge current is:

$$\hat{i}_{k,0} = \frac{U_{dc}}{Z_w} \quad (10)$$

The discharge current is therefore highly determined by the surge impedance of the line. Fig. 5 shows the surge impedance in dependence of the frequency for the cable and overhead line for both configurations. The values of the cable are significantly higher as them of the overhead line, because of the large cable capacitance. For frequencies above 100 Hz the cable surge impedances of both configurations are almost similar. The reason is that the effective series impedances per

unit length Z' for both configurations with grounded sheath are almost identical in the higher frequency range [10]. In case of the overhead lines differences occur between both configurations for Z_w over the whole frequency range, caused by the influence of the earth impedance of the monopolar configuration.

Another important factor which determines the duration of the discharge is the damping constant of the line. The damping constant in dependence of the frequency for the cable and overhead line for both configurations is illustrated in Fig. 6. The cable configurations have distinctively higher damping constants over the whole frequency and for frequencies above 100 Hz the values for the monopolar and bipolar configuration are almost the same. The damping constant of the monopolar overhead line configuration is higher as that of the bipolar configuration because of the reason mentioned above.

For the analysis of the line discharge current the short-circuit current contribution of the converter is neglected in this subsection. The converter is treated as a current source, which corresponds for the travelling wave to an open end. The line with a length of 100 km is charged on a voltage of $U_{dc} = 467$ kV (monopolar) and $U_{dc} = \pm 467$ kV (bipolar), which is the open-circuit voltage of the converter (uncontrolled). The fault resistance is zero.

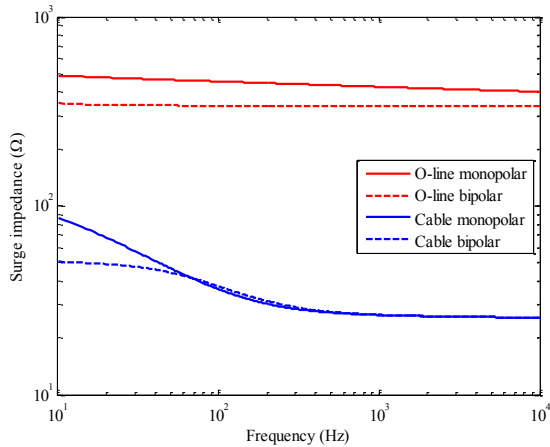


Fig. 5. Surge impedance in dependence of the frequency for the cable and overhead line configuration (monopolar, bipolar).

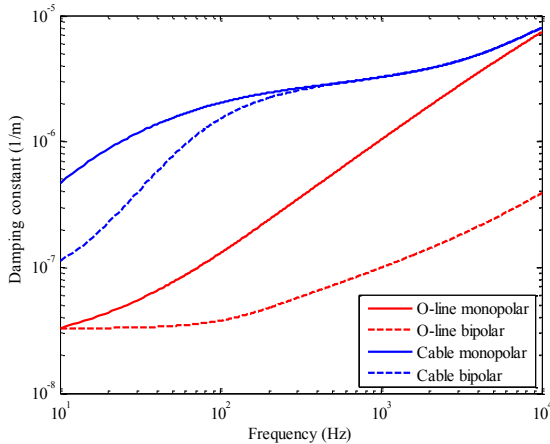


Fig. 6. Damping constant in dependence of the frequency for the cable and overhead line configuration (monopolar, bipolar).

Fig. 7 shows the resulting discharge currents of the cable and overhead line for both configurations. Because of similar characteristic line parameters the cable discharge currents of the monopolar and bipolar configuration are almost equal. The currents have a frequency of 430 Hz, an amplitude of 18 kA and a short-circuit duration below 10 milliseconds. The discharge current amplitudes of the overhead line configurations are significantly smaller because of the larger surge impedances. The initial amplitudes are 1.1 kA and 1.5 kA with frequencies of 650 Hz and 750 Hz respectively. The duration of the discharge for the monopolar configuration is similar to them of the cables because of the high damping constant. In case of the bipolar configuration the discharge duration is comparatively high.

Fig. 7 signifies that the cable discharge current is more important as the current of the overhead line, while analyzing the total short-circuit current. Additionally, the discharge of the line is only relevant in the first few milliseconds after short-circuit occurrence.

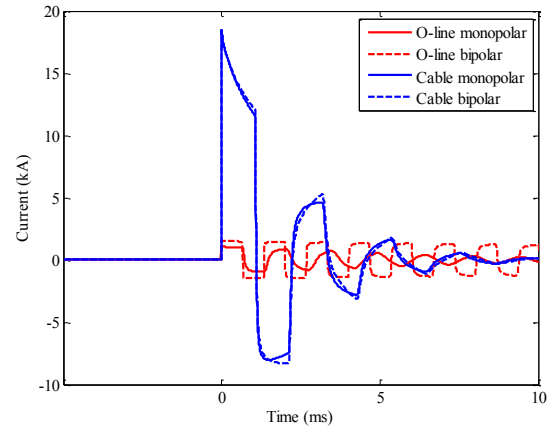


Fig. 7. Time-course of the discharge current of the cable and overhead line for monopolar and bipolar configurations.

IV. SIMULATION

In subsection A the simulation model of the analysis is presented. In subsection B the converter short-circuit currents resulting from frequency-dependent line models are compared to them of lumped line models. Finally in subsection C the effect of the line discharge current on the total short-circuit current is evaluated.

A. Simulation Model

The simulation model consists of an AC system infeed, a converter transformer, an MMC converter in the short-circuit state (blocked IGBTs) and a DC line section between converter terminal and fault location (solid short circuit). The parameters of the simulation model are shown in Table II. The chosen values are similar to them of the INELFE project [11]. For the DC line section either a cable or an overhead line (OHL) is applied based on the parameters in Table I.

The analyses are performed for an MMC in monopolar and bipolar configuration. In case of the monopolar configuration a DC line with earth return is considered.

TABLE II
SIMULATION MODEL PARAMETERS

System infeed	
Nominal voltage U_n	380 kV
Operating voltage U_b	400 kV
Voltage factor c	1.1
Initial short-circuit current I_k''	60 kA
R/X -ratio	0.1
Transformer	
Short-circuit voltage u_{kr}	0.15 p.u.
Ratio U_{rTHV}/U_{rTLV}	400 kV/333 kV
Apparent rated power S_{rT}	1050 MVA
Relative losses u_{Rr}	0.005 p.u.
Converter	
Apparent rated power S_{rC}	1050 MVA
Arm inductance L_a	50 mH

B. Results (uncharged line)

In the following the necessity of using frequency-dependent lines for the evaluation of HVDC converter short-circuit currents is analyzed. For that the results of a frequency-dependent line model from PSCAD are compared to them of a model with lumped elements. The simplified line model – convenient for short-circuit current calculation methods – consists of a series connection of a resistance and an inductance calculated for a single frequency. Shunt capacitances are neglected. At the instance of the short circuit the frequency-dependent line is uncharged to focus only on the short-circuit current contribution of the converter.

The parameters of the simplified line model are calculated for a frequency of 0 Hz and for a frequency of 50 Hz to cover the present frequencies of a converter short-circuit current (see section II). For a monopolar overhead line according to Table I with a section length of 100 km the values are: $R_{0Hz} = 2.24 \Omega$, $L_{0Hz} = 250$ mH, $R_{50Hz} = 7 \Omega$, $L_{50Hz} = 190$ mH. The resulting converter short-circuit currents for the three different line representations (frequency-dependent, 0 Hz and 50 Hz) are shown in Fig. 8 for an MMC in a monopolar configuration. The general time-course is similar to the short-circuit current in Fig. 1 with the difference, that no distinct peak occurs ($i_p = I_k$), because of the large arm and DC line inductance.

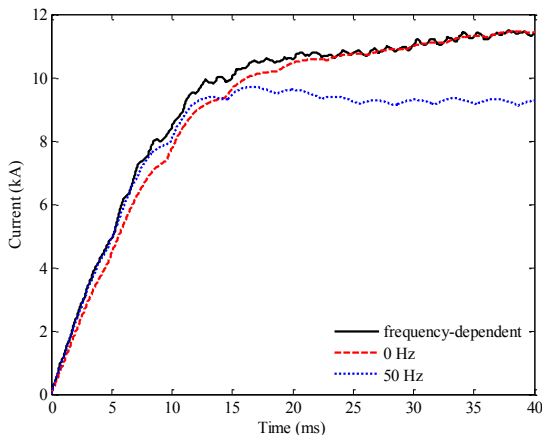


Fig. 8. Converter short-circuit currents for three different line models (frequency-dependent, 0 Hz and 50 Hz).

In the first few milliseconds after short-circuit occurrence the frequency-dependent model is very good represented by the 50-Hz-model. Subsequently, differences occur, because the high resistance R_{50Hz} reduces significantly the amplitude of the peak and steady-state short-circuit current. The 0-Hz-model covers the time-course of the frequency-dependent model after 20 milliseconds very well. Prior to that, differences between simplified and exact model are caused by the higher inductance L_{0Hz} , which decreases the current rising.

The example from above illustrates that the best representation of the short-circuit current for lines with lumped elements depends on the chosen frequency. According to Fig. 3 and Fig. 4 the resistance of the line increases and the inductance decreases with increasing frequency. A conservative approach, which covers the transient as well as the steady-state short-circuit current, is the application of the resistance R_{0Hz} and the inductance L_{50Hz} in combination for a single lumped line model, which have the lowest values in that frequency range respectively.

Fig. 9 shows the short-circuit currents of a frequency-dependent (black curve) and a lumped R_{0Hz}/L_{50Hz} -overhead line model (red curve) in a monopolar MMC configuration. The short-circuit currents are simulated for four different line section lengths: 2 km, 50 km, 100 km and 200 km. In general, the peak short-circuit current decreases and the time to peak increases with increasing distance between converter terminal and fault location. The steady-state short-circuit current is slightly decreased by the increasing DC resistance. At longer line length i_p corresponds to I_k . The current of the simplified model covers the current of the frequency-dependent model in particular in the steady state. In the transient section the results of the simplification are slightly above of them of the exact model, which is convenient from a short-circuit current calculation point of view.

In Fig. 10 the results of the bipolar overhead line configuration are illustrated, which are similar to the previous case. Because of the missing influence of the frequency-dependent earth impedance the differences between exact and simplified model are very low.

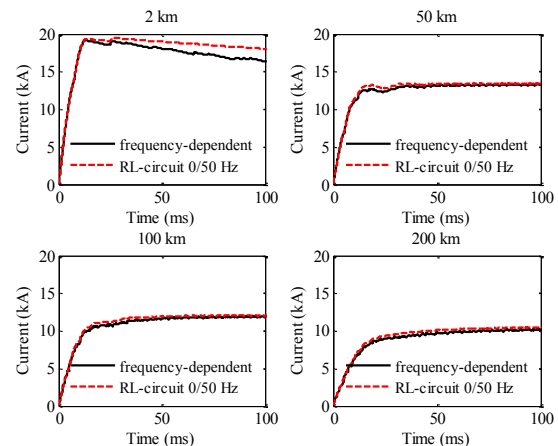


Fig. 9. Short-circuit currents of a frequency-dependent and a simplified OHL-model for different line lengths in a monopolar MMC configuration.

As the line impedance of the bipolar configuration is almost constant in the frequency range of interest (see Appendix Table III), it is also convenient to apply a simplified line model with resistance and inductance calculated for the same frequency.

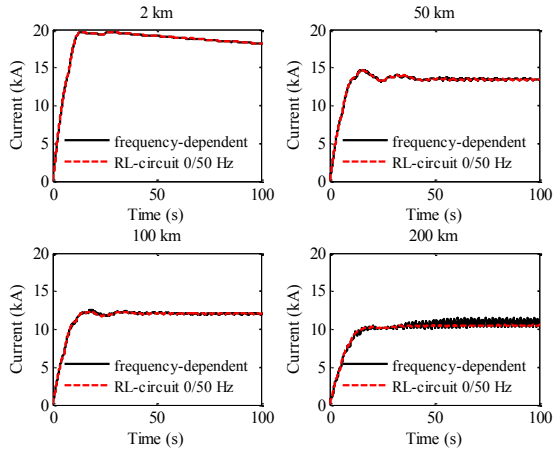


Fig. 10. Short-circuit currents of a frequency-dependent and a simplified OHL-model for different line lengths in a bipolar MMC configuration.

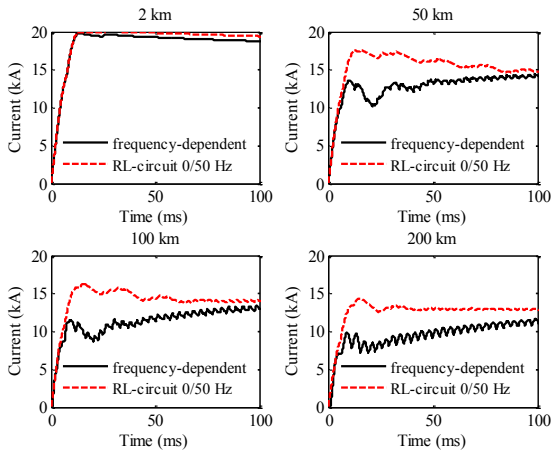


Fig. 11. Short-circuit currents of a frequency-dependent and a simplified cable model for different line lengths in a monopolar MMC configuration.

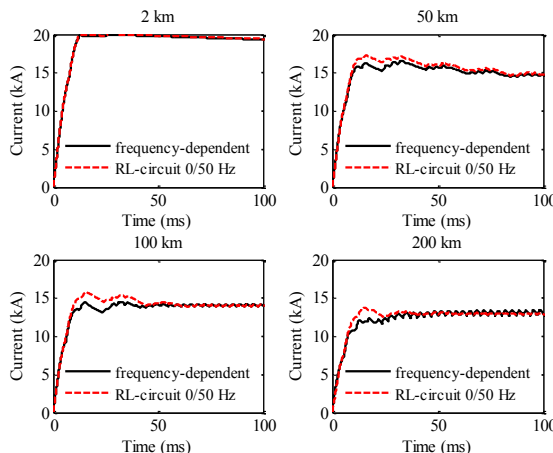


Fig. 12. Short-circuit currents of a frequency-dependent and a simplified cable model for different line lengths in a bipolar MMC configuration.

In case of the monopolar cable configuration the differences in the transient section between the two models are relatively high (see Fig. 11). The peak short-circuit currents of the simplified model are significantly higher in particular for medium line section lengths. The reason is that the inductance of the monopolar cable with grounded sheath at 50 Hz is very low in comparison to the inductance at 0 Hz (see Appendix Table III), which increases the current rise and the peak current in the simplified model. From a short-circuit current calculation point of view it would be more convenient to apply a simplified model with line parameters calculated for 0 Hz, which gives better results for the peak short-circuit current.

The short-circuit current of an MMC with a bipolar cable configuration in Fig. 12 can be represented by the $R_{0\text{Hz}}/L_{50\text{Hz}}$ -model. The peak short-circuit currents are slightly higher for the simplified model. In the bipolar case the differences between the inductances at 0 Hz and 50 Hz are significantly lower.

C. Results (charged line)

In the previous subsection the converter short-circuit current under consideration of an uncharged line is analyzed. In the following the line on the DC side is charged on the open-circuit voltage of the converter ($U_{\text{dc}} = 467$ kV). Only the results of bipolar configurations are shown in this section, as them of monopolar configurations are similar.

In Fig. 13 the converter short-circuit currents with charged and uncharged frequency-dependent overhead line models are compared for different line section lengths. At the occurrence of the short circuit a travelling wave propagates from the fault location and is reflected at the converter terminal. Because of the large arm inductances the converter behaves like an open end for the traveling wave (current reflection factor $r = -1$). Consequently, the general behavior of the discharge current described in section III can be applied to these cases. The discharge current of the line and the converter current according to subsection B are superposed. Fig. 13 illustrates, that between both cases – charged (red curve) and uncharged (black-dashed curve) – only small differences occur in particular for shorter line section lengths.

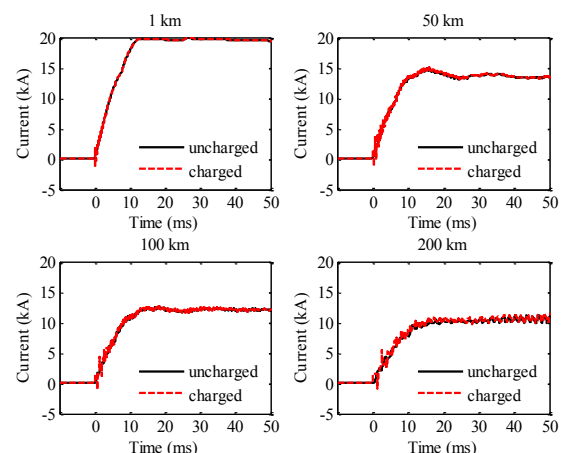


Fig. 13. Short-circuit currents with a charged and uncharged overhead line for different line lengths in a bipolar MMC configuration.

With increasing line length the frequency of the discharge current decreases and consequently the line damping too (see Fig. 6). Therefore, the duration of the line discharge is increased for longer line sections. Because of the high surge impedance of the overhead line the amplitude according to (10) is very low. The discharge current of the overhead line has therefore almost no effect on the total short-circuit current, which is mainly determined by the converter.

For the cable discharge current shown in Fig. 14 applies also the superposition principle described above. In the first instances after short-circuit occurrence the amplitude of the discharge current is significantly higher, because of the smaller surge impedance. In that example the peak short-circuit current is determined by the contribution of the cable. The duration of the discharge is very low caused by the high damping constant of the cable (see Fig. 6). Therefore, the discharge current of the cable has to be considered only in the first few milliseconds.

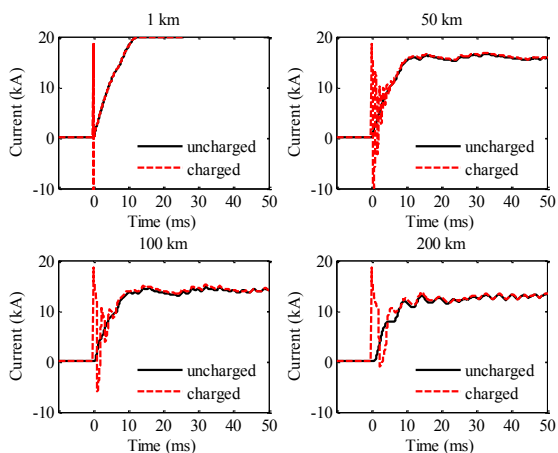


Fig. 14. Short-circuit currents with a charged and uncharged cable for different line lengths in a bipolar MMC configuration.

V. CONCLUSION

For the calculation of HVDC converter short-circuit currents on the DC side it is sufficient to represent the frequency-dependent line by a lumped resistance and inductance in series. The applied frequency depends on the determination of a specific characteristic short-circuit current parameter.

The steady-state short-circuit current is calculated with the DC resistance of the line in all the cases (overhead line/cable, monopolar/bipolar). The line inductance is neglected. The peak short-circuit current and time to peak are calculated with a resistance of 0 Hz and an inductance of 50 Hz in case of the monopolar/bipolar overhead line and the bipolar cable. The resistance and inductance of a monopolar cable with grounded sheath should be both determined at a frequency of 0 Hz.

The discharge current of the DC line can be calculated separately and superposed with the converter short-circuit current. Because of the high surge impedance of the overhead line the discharge current has no relevance for the total short-circuit current. The amplitude of the cable discharge current is

significantly higher because of the small surge impedance. The discharge current can be neglected after 10 milliseconds, caused by the high damping constant of the cable.

The results obtained in this paper apply also to larger HVDC grids with radial and meshed topologies. Future work should focus on the mutual interaction between several converters at a short circuit on the DC side.

VI. APPENDIX

TABLE III
LINE PARAMETERS

Length		2 km	50 km	100 km	200 km
Overhead line monopolar	$R_{0\text{Hz}}$	0.045 Ω	1.12 Ω	2.24 Ω	4.5 Ω
	$R_{50\text{Hz}}$	0.14 Ω	3.5 Ω	7 Ω	13.76 Ω
	$L_{0\text{Hz}}$	5 mH	125 mH	250 mH	500 mH
	$L_{50\text{Hz}}$	3.8 mH	94 mH	188 mH	373 mH
Overhead line bipolar	$R_{0\text{Hz}}$	0.083 Ω	2.23 Ω	4.47 Ω	8.93 Ω
	$R_{50\text{Hz}}$	0.093 Ω	2.32 Ω	4.63 Ω	9.15 Ω
	$L_{0\text{Hz}}$	4.1 mH	101 mH	203 mH	406 mH
	$L_{50\text{Hz}}$	4.1 mH	101 mH	202 mH	402 mH
Cable monopolar	$R_{0\text{Hz}}$	0.0147 Ω	0.368 Ω	0.737 Ω	1.47 Ω
	$R_{50\text{Hz}}$	0.25 Ω	6.21 Ω	12.3 Ω	23.3 Ω
	$L_{0\text{Hz}}$	5.5 mH	137 mH	275 mH	550 mH
	$L_{50\text{Hz}}$	0.5 mH	12 mH	24 mH	50 mH
Cable bipolar	$R_{0\text{Hz}}$	0.029 Ω	0.7252 Ω	1.45 Ω	2.9 Ω
	$R_{50\text{Hz}}$	0.26 Ω	6.47 Ω	12.7 Ω	23.5 Ω
	$L_{0\text{Hz}}$	2.1 mH	52.3 mH	105 mH	209 mH
	$L_{50\text{Hz}}$	1.4 mH	36 mH	71.5 mH	139 mH

VII. REFERENCES

- [1] V. Akhmatov, M. Callavik, C. M. Franck, S. E. Rye, T. Ahndorf, M. K. Bucher, H. Müller, F. Schettler and R. Wiget, "Technical Guidelines and Prestandardization Work for First HVDC Grids," *IEEE Trans. Power Delivery*, vol. 29 no. 1, pp. 327-335, Feb. 2014.
- [2] *Short-circuit currents in three-phase AC systems – Part 0: Calculation of short-circuit currents*, IEC Standard 60909-0, April 2002.
- [3] R. Marquardt, "Modular Multilevel Converter: An universal concept for HVDC-Networks and extended DC-Bus-applications," in *Proc. 2010 IEEE International Power Electronics Conference*, pp. 502-507.
- [4] R. Marquardt, "Modular Multilevel Converter Topologies with DC-Short Circuit Current Limitation," in *Proc. 2011 IEEE International Conference on Power Electronics – ECCE Asia*, pp. 1425-1431.
- [5] Manitoba HVDC Research Centre, *PSCAD User's Guide*, 2010 pp. 273-317.
- [6] *Short-circuit currents – Short-circuit currents in d.c. auxiliary installations in power plants and substations –Part 1: Calculation of short-circuit currents*, IEC Standard 61660-1, June 1998.
- [7] A. Wasserrab and G. Balzer, "Determination of DC Short-Circuit Currents of MMC-HVDC Converters for DC Circuit Breaker Dimensioning," presented at the 11th IET Int. Conf. on AC and DC Power Transmission, Birmingham, UK, 2015.
- [8] L. Hofmann, "Modeling of Overhead Wires with Frequency-dependent Parameters in Short-term Range," Ph.D. dissertation, Div. of Power Supply, Univ. Hannover, Germany, 1998.
- [9] L. M. Wedepohl and D. J. Wilcox, "Transient analysis of underground power-transmission systems," in *Proc. IEE*, vol. 120, no. 2, pp. 253-260, Feb. 1973.
- [10] A. Wasserrab and G. Balzer, "Frequency-dependent cables for the calculation of line short-circuit currents in HVDC networks," in *Proc. 2014 IEEE 49th International Universities Power Engineering Conference*.
- [11] S. Dennetière, S. Nguéfeu, H. Saad and J. Mahseredjian, "Modeling of Modular Multilevel Converters for the France-Spain link," in *Proc. 2013 International Conference on Power Systems Transients*.